

Surface Interaction Forces of Well-Defined, High-Density Polymer Brushes Studied by Atomic Force Microscopy. 2. Effect of Graft Density

Shinpei Yamamoto, Muhammad Ejaz, Yoshinobu Tsujii, and Takeshi Fukuda*

Institute for Chemical Research, Kyoto University, Uji, Kyoto 611-0011, Japan

Received November 29, 1999

ABSTRACT: Poly(methyl methacrylate) (PMMA) brushes with the same chain length but different graft densities were prepared on a silicon substrate by the surface-initiated atom transfer radical polymerization technique. The graft density σ was changed in a wide range extending to an exceptionally high value ($0.07 < \sigma$ (chains/nm²) < 0.7) by photodecomposing the surface-fixed initiator, 2-(4-chlorosulfonylphenyl)-ethyltrichlorosilane (CTCS). The surface density σ_i of CTCS was determined by the grazing-angle reflection–absorption FT-IR measurement. The comparison of σ and σ_i suggests that there is a limiting value in σ that cannot be exceeded even if σ_i is increased. The direct force measurements were made at the brush surface swollen in toluene by an atomic force microscope with a silica particle-attached cantilever. The analysis of the obtained force–distance profiles revealed that the equilibrium thickness L_e scaled by the full chain length L_c varies such as $L_e/L_c \propto \sigma^n$ with n increasing from about 0.3 to 0.5 with increasing σ and that the brush with a higher σ is more resistant to compression. These results are poorly explained by the scaling theory, which was derived for “moderately dense” brushes. This suggests that the studied σ range is in the “high-density” regime, in which higher-order interactions among graft chains are important.

Introduction

Polymers densely end-grafted on a solid surface will be obliged to stretch away from the surface, forming the so-called “polymer brush”. Because of their importance in many areas of science and technology, e.g., colloid stabilization, adhesion, lubrication, tribology, and rheology,^{1–5} polymer brushes in a solvent have been extensively studied by a surface force apparatus (SFA),^{6–9} an atomic force microscope (AFM),^{10–13} neutron reflectometry,^{14,15} and so on. Most of the polymer brushes experimentally studied so far were prepared by end-functionalized polymers or block copolymers with the terminal group or one of the blocks selectively adsorbed on the surface. These systems had a rather low graft density, typically 0.001–0.05 chains/nm², corresponding to the “moderately dense” regime in which graft chains overlap each other but the volume fraction of polymer in the layer is still low.

Recently, we succeeded in preparing low-polydispersity poly(methyl methacrylate) (PMMA) brushes with an exceptionally high graft density. AFM force measurements revealed that these polymer brushes have properties quite different and unpredictable from the “moderately dense” polymer brushes previously studied. Most notably, the chains in these high-density brushes were highly extended, nearly to their full lengths, and highly resistant against compression.¹⁶ We believe that these were virtually the first observations of the “real” polymer brush behavior. A key technology to this success was the use of living radical polymerization (LRP)¹⁷ along with a high-efficiency initiator fixed on the substrate.^{16a}

In this work, we have made AFM force measurements in toluene on a series of PMMA brushes with nearly the same chain length but different graft densities. These samples were prepared by the atom transfer radical

polymerization (ATRP) technique,¹⁸ the powerful variant of LRP used in the previous work.¹⁶ The graft density could be widely changed by photodecomposing the initiator that had been fixed on the substrate. In what follows, we will discuss the effect of graft density on the structure and interaction forces of polymer brushes swollen in a good solvent. This work will hopefully give a comprehensive picture of polymer brushes with varying graft densities from low to extremely high values throughout.

Experimental Section

Preparation and Characterization of Initiator-Fixed Substrates. To immobilize the initiator, 2-(4-chlorosulfonylphenyl)ethyltrichlorosilane (CTCS) (Gelest, Inc., USA), a silicon wafer or a SiO₂/Au/Cr-coated glass plate was immersed in an anhydrous toluene solution of CTCS (ca. 1.0 wt %) for 2 h, washed with tetrahydrofuran, and then dried. The silicon wafer is usually covered with a silicon oxide layer, and in the solution, the chlorosilyl group of CTCS reacts with the silanol group on the substrate surface, forming a Si–O–Si covalent bond. To adjust the density of the initiator, the CTCS-fixed substrate was irradiated for various periods of time through a quartz diffuser by a high-pressure mercury lamp (Toshiba H-400P). The photodecomposition reaction of CTCS was monitored by means of grazing-angle reflection–absorption infrared (GIR) spectroscopy. To enhance the intensity of the reflection beam in the GIR measurements, the SiO₂/Au/Cr-coated substrate was used. This substrate was prepared as follows: a 5 nm thick Cr layer and then a 100 nm thick Au layer were vacuum-evaporated on a cleaned glass plate, on top of which a 5–10 nm thick SiO₂ layer was deposited by a reactive evaporation of silicon monoxide in the presence of 10^{–4} Torr of oxygen. The Cr layer was used for the improvement of adhesion between the glass surface and the gold layer. GIR measurements were carried out on a BioRad FTS-6000 Fourier transform spectrometer equipped with a reflection accessory and a liquid-nitrogen-cooled MCT detector. p-Polarized light was used at an incident angle of 80°.

Preparation and Characterization of Polymer Brushes. The PMMA brushes were prepared by the surface-initiated ATRP technique:^{16a} silicon wafers on which CTCS was fixed

* To whom correspondence should be addressed: e-mail fukuda@scl.kyoto-u.ac.jp.

Table 1. Characteristics of the PMMA Brushes^a

sample	L_d^b (nm)	L_e^c (nm)	σ (chains/nm ²)
C1	5	56	0.07
C2	11	71	0.14
C3	32	119	0.42
C4	55	156	0.70

^a $M_n = 56\,700$ and $M_w/M_n = 1.26$; these values are for the free polymer produced in solution (see text). ^b Thickness in dry state. ^c Equilibrium thickness in toluene at room temperature (about 25 °C).

with differing densities were subjected to the graft polymerization at 90 °C for 6 h in a degassed diphenyl ether solution containing CuBr (10 mM), 4,4'-di-*n*-heptyl-2,2'-bipyridine (20 mM), methyl methacrylate (4.7 M), and *p*-toluenesulfonyl chloride (TsCl, 4.8 mM). TsCl was added as a free initiator not only to control the polymerization but also to yield free polymers, which are useful as a measure of the molecular weight and molecular weight distribution of the graft chains.^{16a} After polymerization, the substrates were rinsed in a Soxhlet extractor with toluene for 12 h to remove physisorbed polymers and impurities. The thickness L_d of the polymer layer in a dry state was determined by ellipsometry (a DVA ellipsometer, Mizojiri Optical Co., Ltd., Japan).

The characteristics of the PMMA brushes (C1–C4), prepared in the same pot, are summarized in Table 1. In the table, the number-average molecular weight (M_n) and the polydispersity index (M_w/M_n) are those of the free polymers produced in the solution, as determined by the PMMA-calibrated gel permeation chromatographic (GPC) analysis. There are reasons to believe that these values should well approximate those of the graft chains.^{16,19} The graft density σ was calculated from L_d , M_n , and the bulk density of a PMMA film (1.19 g/cm³).²¹

AFM Measurements. Topographic imaging and force measurements were performed by an atomic force microscope (Seiko Instruments Inc., Japan, SPI3600) with a V-shaped cantilever (Olympus Optical Co., Ltd., Japan, spring constant 0.16 N/m). The spring constants of several cantilevers were measured according to the method of Cleaveland et al.,²² and the obtained values were found to be within $\pm 10\%$ of the company-given value. A liquid cell was used for the measurement in toluene, a good solvent for PMMA, at room temperature (about 25 °C). Toluene (Spectrograde, Dojindo Laboratories, Japan) was used without further purification. Interaction forces between the PMMA brush and the silica sphere (Ube Nitto Kasei, Japan, diameter 10 μ m) attached to the cantilever as a probe were measured in toluene as a function of the separation using a modified SPI3600 AFM apparatus, in which a piezo actuator of the one-dimensional layered type (Taiheiyo Cement, Co., Japan, PMF-2020 controlled by the piezo driver PM-1100) was installed, and its hysteresis behavior was corrected by simultaneously measuring its piezo current. Details of the force measurement were described elsewhere.^{16b} Typically, force curves were collected with a scan rate of 0.5 Hz, and a total of 60 force curves were taken at different locations on each sample. Immediately prior to each force measurement, the silica probe fixed on the cantilever was immersed in a solution of dimethyldichlorosilane/toluene (1:3 by weight) for 30 min to make the surface hydrophobic. A hydrophobically treated silicon wafer was also prepared in the same way.

The raw AFM force data (cantilever deflection vs displacement data) were converted into the reduced force (F/R , see below) vs separation (D) relation following the principle of Ducker et al.²³ The zero of D is defined as the location of the so-called "constant compliance" plane beyond which the sample was no more compressible. For a low-density polymer brush, this plane approximately coincides with the substrate surface. For a high-density system with a thick polymer layer, however, the distance (the "offset distance" D_0) between the $D = 0$ plane and the substrate surface can be very large. The difficulty of determining D_0 had been a problem in the AFM force measurement. We could determine D_0 by scratching the polymer layer and AFM-scanning across the scratch boundary.^{16b} The

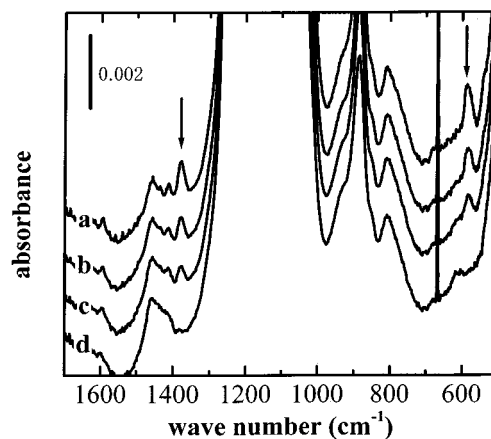


Figure 1. GIR spectra of the CTCS-fixed substrates, irradiation time = (a) 0 min, (b) 1 min, (c) 2 min, and (d) 20 min.

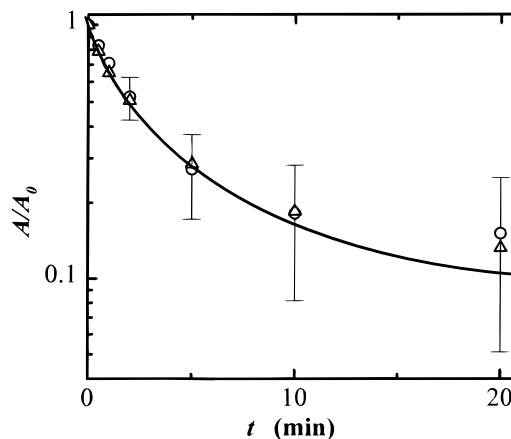


Figure 2. Plots of relative absorbance A/A_0 of the S=O stretching band vs irradiation time t for CTCS-fixed substrates. Data obtained by different experiments are represented by different symbols showing reproducibility.

true distance D between the surfaces of the substrate and the probe sphere may be given by

$$D = D' + D_0 \quad (1)$$

Results and Discussions

Photodecomposition of Initiator and Graft Density. The CTCS fixed on the substrate was irradiated by UV light. Figure 1 shows GIR spectra of the irradiated and unirradiated samples. Two absorption bands characteristic of the chlorosulfonyl group of CTCS were observed at wavenumbers of 1380 cm⁻¹ and 580 cm⁻¹. Both peaks decreased with increasing irradiation time t , which confirms that the chlorosulfonyl group, the initiating group for ATRP, was photodecomposed by UV irradiation. In Figure 2, the relative absorbance A/A_0 of the S=O asymmetric stretching band (1380 cm⁻¹) was plotted against t , where A_0 and A are the absorbances at $t = 0$ (unirradiated) and t , respectively. This ratio A/A_0 corresponds to the survival ratio σ_t/σ_0 of the initiating group, where σ_0 and σ_t are the surface densities of the fixed initiator at $t = 0$ (unirradiated) and t , respectively.

The irradiated and the unirradiated samples were subjected to the ATRP under the same polymerization conditions. The AFM observation in the air revealed the formation of a homogeneous graft polymer layer on the substrate. The dry thickness L_d of the graft polymer layer decreased with increasing irradiation time t . The

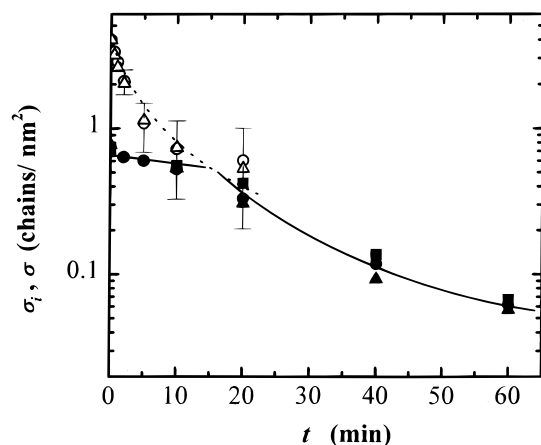


Figure 3. Plots of surface density σ_i and σ vs irradiation time t . The open symbols represent σ_i . The closed symbols represent σ . Data obtained by different experiments are represented by different symbols showing reproducibility.

free polymers produced from the free initiator TsCl in the solution had nearly the same M_n in all cases. According to the previous results,^{16,19} this indicates that all the samples have graft chains with nearly the same M_n . Therefore, the decrease in L_d may be ascribed to the decrease in graft density σ . The σ values, calculated from L_d and M_n , were plotted against t in Figure 3. The figure also shows the variation of σ_i , which was calculated with the relation $\sigma_i = \sigma_0(A/A_0)$ by assuming $\sigma_0 = 4$ molecules/nm² (the experimental value for the monolayer of 2-(4-chlorosulfonylphenyl)ethyltrimethoxysilane on a water surface). The ratio σ/σ_i gives the graft efficiency of the fixed initiator. For the unirradiated sample, σ/σ_i is approximately 0.2. Clearly, this rather low efficiency is to be ascribed to a steric effect in the surface-graft polymerization: if, for example, $\sigma/\sigma_i = 1$ and hence $\sigma = 4$, the density of the graft layer is estimated to exceed 2.7 g/cm³, which is totally unrealistic as compared with the bulk density of PMMA (1.19 g/cm³). As Figure 3 shows, σ_i rapidly decreases with increasing irradiation time t , but σ stays nearly constant at the beginning, meaning a rapid increase in the efficiency σ/σ_i . The figure suggests that the σ and σ_i curves get in touch with each other at $t \approx 15$ min. Although σ_i for $t > 20$ min could not be determined with meaningful accuracy, it is likely that σ and σ_i go together, i.e., $\sigma/\sigma_i \approx 1$ for $t > 15$ min. The high graft efficiency (nearly 100% for low values of σ_i) suggested here is consistent with the generally high initiation efficiency ($\sim 100\%$) in free ATRP runs.

No characteristic structure was observed by AFM on the surfaces of the irradiated substrates either before or after graft polymerization, suggesting that the fixed initiators are randomly photodecomposed by the UV irradiation, and hence the graft chains are randomly distributed on the surface. The steric interactions between neighboring chains could possibly produce a certain correlation in their relative positions on the surface, but such details are difficult to study at this time.

Force–Distance Profile of Polymer Brush. The surface interaction forces of the solvent-swollen PMMA brushes compressed by the probe sphere were measured in toluene. The measured force F can be reduced to the free energy G_f of interactions between two parallel plates according to the Derjaguin approximation,

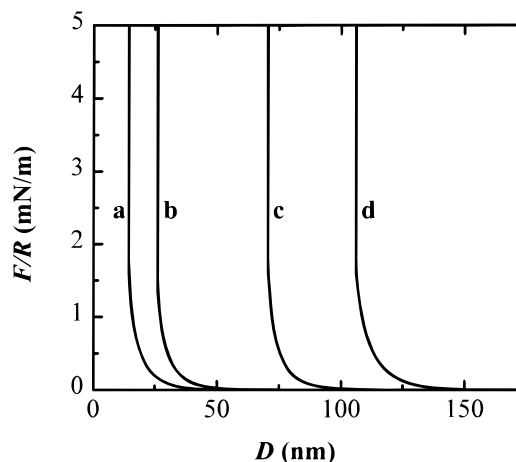


Figure 4. Advancing-mode force profiles (F/R vs D curves) of the PMMA brushes, (a) C1, (b) C2, (c) C3, and (d) C4. These force profiles are the averaged ones.

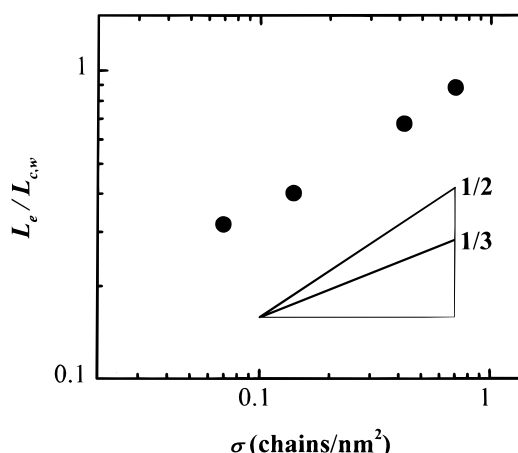


Figure 5. Plots of $L_e/L_{c,w}$ vs graft density σ , where $L_{c,w}$ is the weight-average chain length (see text).

$F/R = 2\pi G_f$, where R is the radius of the probe sphere. Figure 4 shows the F/R vs separation D profiles (force curves) measured in the advancing mode (the probe sphere approaching the brush). Note that D is the corrected distance according to eq 1. Essentially no interaction force was observed for the bare silicon substrate. At the brush surfaces, repulsive forces were observed, which originate from the steric interaction between the solvent-swollen PMMA brush and the probe sphere. The force curve strongly depended on the graft density: the higher was the graft density, the larger was the separation where the interactions are observed. This clearly shows that the graft chains get more and more extended as the graft density is increased.

Equilibrium Thickness of Polymer Brush. Figure 5 shows the plot of $\log(L_e/L_{c,w})$ vs $\log \sigma$, where L_e is the equilibrium thickness of the swollen brush, defined as the critical distance from the substrate surface beyond which no repulsive force was detectable, and $L_{c,w}$ is the full length of the graft chain in the all-trans conformation. The subscript w indicates the weight-average length

$$L_{c,w} = (M_w/M_0)l_0 \quad (2)$$

where M_0 is the molecular weight of the monomer unit and l_0 is the length per monomer unit ($l_0 = 0.25$ nm for PMMA). The weight average, rather than the number

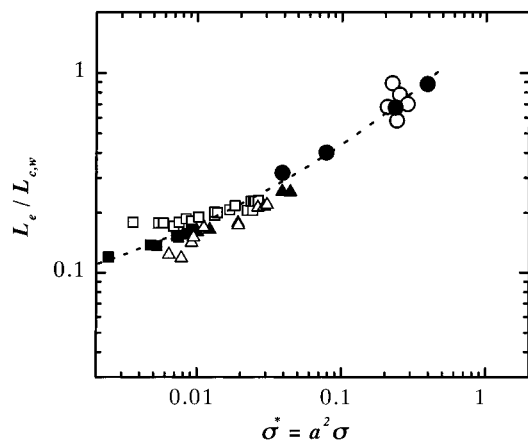


Figure 6. Plots of $L_e/L_{c,w}$ vs dimensionless graft density $\sigma^* = a^2\sigma$ (see text); (1) PS-poly(dimethylsiloxane) block copolymers: \square ($M_{w,PS} = 60\,000$) and \blacksquare ($M_{w,PS} = 169\,000$).²⁶ (2) PEO-PS block copolymers: \triangle ($M_{w,PEO} = 30\,800$) and \blacktriangle ($M_{w,PEO} = 19\,600$).^{27a} (3) PMMA brushes: \circ ($M_w = 31\,300$ – $267\,400$)^{16b} and \bullet ($M_w = 71\,400$, this work).

average, was adopted by referring to the studies of Milner et al.,²⁴ in which a (moderate-density) polymer brush with a *uniform* distribution in chain length ($M_w/M_n > 1$) was predicted to be thicker than the equivalent monodisperse brush with the same M_n by a factor of $1 + \{3/4(M_w/M_n - 1)\}^{1/2}$. According to this relation, our brushes can be approximated with an error of about 10% in L_e by monodisperse brushes with a chain length M_w .

Figure 5 here shows that $L_e/L_{c,w}$ increases with increasing σ , meaning that the graft chains get more and more extended as the graft density increases. For highest-density brush (sample C4) with $\sigma = 0.7$ chains/nm², which is the highest ever reported density, the value of $L_e/L_{c,w}$ even approaches 0.9. Quantitatively, this surprisingly large value may be subject to some ambiguities arising from the indirect estimate of M_w and M_n and the just-mentioned correction for the polydispersity effect, but it certainly indicates that the graft chains in this brush are extended to an extraordinarily high extent, well comparable with fully extended chains.

According to the scaling theory,²⁵ L_e varies like

$$L_e \propto L_c \sigma^{1/3} \quad (3)$$

This relation was derived for the “moderate density” regime and seems to be compatible with the reported experiments in this regime.^{26,27} However, it cannot be expected to be applicable to the present “high-density” brushes. In fact, the slope of the curve in Figure 5 is much larger than $1/3$. It seems to increase with increasing σ , even though this cannot be concluded due to the lack of sufficient number of data points. The previous study on the high-density PMMA brushes ($\sigma \approx 0.4$ chains/nm²) with varying chain lengths has established the approximate proportionality of L_e to L_c .^{16b} Thus, our results on the high-density brushes can be represented by

$$L_e \propto L_c \sigma^n \quad (4)$$

with $n \approx 0.4$ on the average but possibly increases with increasing σ . An increase of n in the high-density regime has been predicted by the theory in which higher-order interactions were taken into account.²⁸

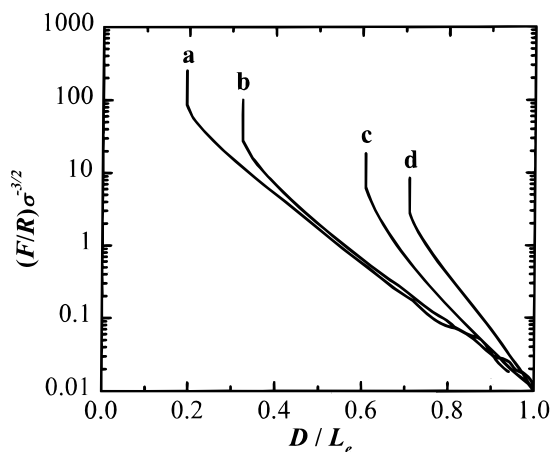


Figure 7. Advancing-mode force profiles replotted in the form of $(F/R)\sigma^{-3/2}$ vs D/L_e in semilogarithm: (a) C1, (b) C2, (c) C3, and (d) C4.

Figure 6 shows the plot of $\log(L_e/L_{c,w})$ vs $\log \sigma^*$ for various kinds of polymer brushes. Here σ^* is the dimensionless surface density

$$\sigma^* = a^2 \sigma \quad (5)$$

where a^2 is the cross-sectional area per monomer unit given by $a^2 = v_0/l_0$ with v_0 being the molecular volume per monomer unit and l_0 being the chain length per monomer unit as before ($l_0 = 0.25$ nm for polystyrene (PS) and 0.365 nm for poly(ethylene oxide) (PEO))²⁹. In this plot, thin polymers such as PEO and thicker polymers such as PS and PMMA could more reasonably be compared. As Figure 6 shows, all the data points approximately form a single curve with a downward curvature. The slope of the curve seems to increase from about 0.2 in the low σ^* region up to about 0.5 in the high σ^* region, thus providing a rather comprehensive view of polymer brushes in the moderate- and high-density regimes. It remains to be answered whether the slope of the curve will still become steeper at higher σ^* region, as the theory²⁸ predicts.

Compressibility of Polymer Brush. Using the scaling approach, de Gennes³⁰ derived the following equation concerning the interaction force f between two parallel plates with a moderately dense polymer brush layer:

$$f(D) \propto \sigma^{3/2} [(L_e/D)^{9/4} - (D/L_e)^{3/4}] \quad (6)$$

where $2L_e$ in the original formulation was replaced by L_e because only one surface was covered by the brush layer in our case. This equation is integrated from L_e to D , giving the interaction free energy G_f between two parallel plates, which is related to the measured F/R values according to the Derjaguin approximation:

$$F/R = 2\pi G_f = 2\pi \int_{L_e}^D f(D) dD \quad (7)$$

Equations 6 and 7 predict that the $(F/R)\sigma^{-3/2}$ value should be scaled by D/L_e .

Figure 7 shows the $(F/R)\sigma^{-3/2}$ vs D/L_e plot for our system. This figure indicates that our system is poorly represented by the scaling theory. In other words, the force–distance profile strongly depends on the graft density. With increasing σ , the scaled force curve becomes steeper, meaning that the brush layer is more

resistant to compression. For example, the brush layer with the highest σ (C4) was compressible only to $D/L_e \approx 0.7$, in contrast to $D/L_e \approx 0.2$ for the lowest one (C1). The theory on "dense" polymer brushes does predict the force curve to become steeper with increasing σ .²⁸

Combined with the results in our previous paper, we conclude that a high-density polymer brush is more and more difficult to be compressed, as either σ or L_e or both increase. This strong resistance against compression might also be related to the dynamic properties of polymer brushes, which will be the topic of a forthcoming paper.

Conclusions

This study has revealed the following: (i) CTCS, fixed on the substrate surface, can be randomly decomposed by UV irradiation. The surface-initiated ATRP on the irradiated substrates gives PMMA brushes with graft densities differing in a wide range. (ii) The equilibrium thickness L_e of the brushes in toluene is scaled as $L_e \propto L_{c,w}\sigma^n$ with $n = 0.3-0.5$ in the range of $0.07 < \sigma < 0.7$. This high exponent n , higher than predicted for "moderately dense" brushes by the scaling theory ($L_e \propto \sigma^{1/3}$), is characteristic of "high-density" brushes. (iii) The repulsive force rapidly increases with decreasing separation, and the force-separation profiles are not scaled by the $(F/R)\sigma^{-3/2}$ vs D/L_e plot predicted for "moderate-density" brushes but dependent on the graft density. The brush with a higher graft density is more resistant to compression; for example, the brush with the highest studied σ ($\sigma = 0.7$) was compressible only to $D/L_e \approx 0.7$, in contrast to $D/L_e \approx 0.2$ for the lowest studied one ($\sigma = 0.07$).

Acknowledgment. The Research Fellowship of the Japan Society for the Promotion of Science for Young Scientists is gratefully acknowledged for partial financial support.

References and Notes

- Napper, D. H. *Polymeric Stabilization of Colloidal Dispersions*; Academic Press: London, 1983.
- Raphaël, E.; de Gennes, P. G. *J. Phys. Chem.* **1992**, *96*, 4002.
- Klein, J. *Ann. Rev. Mater. Sci.* **1996**, *26*, 581.
- Klein, J.; Kumacheva, E. *Science* **1995**, *269*, 816.
- Parnas, R. S.; Cohen, Y. *Rheol. Acta* **1994**, *33*, 485.
- (a) Hadzioannou, G.; Granick, S.; Patel, S.; Tirrell, M. *J. Am. Chem. Soc.* **1986**, *108*, 2869. (b) Watanabe, H.; Tirrell, M. *Macromolecules* **1993**, *26*, 6455.
- Ansarifer, A.; Luckham, P. F. *Polymer* **1988**, *29*, 329.
- Taunton, H. J.; Toprakcioglu, C.; Fetters, L.; Klein, J. *Macromolecules* **1990**, *23*, 571.
- Belder, G. F.; ten Brike, G.; Hadzioannou, G. *Langmuir* **1997**, *13*, 4102.
- Courvoisier, A.; Isel, F.; François, J.; Maaloum, M. *Langmuir* **1998**, *14*, 3727.
- Overney, R.; Leta, D.; Pictroski, C.; Rafailovich, M.; Liu, Y.; Quinn, J.; Sokolov, J.; Eisenberg, A.; Overney, G. *Phys. Rev. Lett.* **1996**, *76*, 1272.
- Kelley, T. W.; Schorr, P. A.; Johnson, K. D.; Tirrell, M.; Frisbie, C. D. *Macromolecules* **1998**, *31*, 4297.
- O'Shea, S. J.; Welland, M. E.; Rayment, T. *Langmuir* **1993**, *9*, 1826.
- (a) Field, J. B.; Toprakcioglu, C.; Ball, R. C.; Dtanley, H. B.; Dai, L.; Barford, W.; Penfold, J.; Hamilton, W. *Macromolecules* **1992**, *25*, 434. (b) Field, J. B.; Toprakcioglu, C.; Dai, L.; Hadzioannou, G.; Smith, G.; Hamilton, W. *J. Phys. II* **1992**, *2*, 2221.
- Anastassopoulos, D. L.; Vradis, A. A.; Toprakcioglu, C.; Smith, G. S.; Dai, L. *Macromolecules* **1998**, *31*, 9369.
- (a) Ejaz, M.; Yamamoto, S.; Ohno, K.; Tsujii, Y.; Fukuda, T. *Macromolecules* **1998**, *31*, 5934. (b) Yamamoto, S.; Ejaz, M.; Tsujii, Y.; Matsumoto, M.; Fukuda, T. *Macromolecules* **2000**, *33*, 5602 (part 1 of this series of papers).
- (a) Moad, G.; Rizzardo, E.; Solomon, D. H. In *Comprehensive Polymer Science*; Eastmond, G. C., Ledwith, A., Russo, S., Sigwalt, P., Eds.; Pergamon: London, 1989; Vol. 3, p 141. (b) Georges, M. K.; Vereg, R. P. N.; Kazmaier, P. M.; Hamer, G. K. *Trends Polym. Sci.* **1994**, *2*, 66. (c) Matyjaszewski, K.; Gaynor, S.; Greszt, D.; Mardare, D.; Shigemoto, T. *J. Phys. Org. Chem.* **1995**, *8*, 306. (d) Moad, G.; Solomon, D. H. *The Chemistry of Free Radical Polymerization*; Pergamon: Oxford, UK, 1995; p 335. (e) Davis, T. P.; Haddleton, D. M. In *New Methods of Polymer Synthesis*; Ebdon, J. R., Eastmond, G. C., Eds.; Blackie: Glasgow, UK, 1995; Vol. 2, p 1. (f) Hawker, C. J. *Trends Polym. Sci.* **1996**, *4*, 183. (g) Colombani, D. *Prog. Polym. Sci.* **1997**, *22*, 1649. (h) *Controlled Radical Polymerization*; Matyjaszewski, K., Ed.; ACS Symposium Series 685; American Chemical Society: Washington, DC, 1998. (i) Sawamoto, M.; Kamigaito, M. In *Polymer Synthesis*; Materials Science and Technology Series; VCH-Wiley: Weinheim 1998; Chapter 1. (j) Otsu, T.; Matsumoto, A. *Adv. Polym. Sci.* **1998**, *136*, 75. (k) Fukuda, T.; Goto, A.; Ohno, K. *Macromol. Rapid Commun.* **2000**, *21*, 151.
- (a) Wang, J. S.; Matyjaszewski, K. *J. Am. Chem. Soc.* **1995**, *117*, 5614. (b) Kato, M.; Kamigaito, M.; Sawamoto, T.; Higashimura, T. *Macromolecules* **1995**, *28*, 1721. (c) Percec, V.; Barboiu, B. *Macromolecules* **1995**, *28*, 7970. (d) Granel, C.; Dubois, Ph.; Jérôme, R.; Teyssié, Ph. *Macromolecules* **1996**, *29*, 8576. (e) Haddleton, D. M.; Jasieczek, C. B.; Hannon, M. J.; Scooter, A. J. *Macromolecules* **1997**, *30*, 2190. (f) Leduc, M. R.; Hayes, W.; Fréchet, J. M. J. *J. Polym. Sci., Part A: Polym. Chem.* **1998**, *36*, 1. (g) Jankova, K.; Chen, X.; Kops, J.; Batsberg, W. *Macromolecules* **1998**, *31*, 538. (h) Angot, S.; Murthy, K. S.; Taton, D.; Gnanou, Y. *Macromolecules* **1998**, *31*, 7218. (i) Ohno, K.; Goto, A.; Fukuda, T.; Xia, J.; Matyjaszewski, K. *Macromolecules* **1998**, *31*, 2699.
- In more recent work,²⁰ methyl methacrylate was graft-polymerized on initiator-fixed silica particles with a large surface area, and the direct GPC analysis of the graft chains cleaved off the silica particles by treatment with a HF solution confirmed that the graft chains have nearly the same molecular weight and molecular weight distribution as the free polymers.
- (a) Yamamoto, S.; Ejaz, M.; Ohno, K.; Tsujii, Y.; Matsumoto, M.; Fukuda, T. *ACS Polym. Prepr.* **1999**, *40*, 401. (b) Marumoto, Y.; Ejaz, M.; Ohno, K.; Tsujii, Y.; Fukuda, T.; Miyamoto, T. *Polym. Prepr., Jpn.* **1999**, *48*, 139.
- Brandrup, J.; Immergut, E. H., Eds. *Polymer Handbook*; John Wiley & Sons: New York, 1989.
- Cleaveland, J. P.; Manne, S.; Bocek, D.; Hansma, P. K. *Rev. Sci. Instrum.* **1993**, *64*, 403.
- Ducker, W. A.; Sendan, T. J.; Pashley, R. M. *Langmuir* **1992**, *8*, 1831.
- (a) Milner, S. T. *Europhys. Lett.* **1988**, *7*, 695. (b) Milner, S. T.; Witten, T. A.; Cates, M. E. *Macromolecules* **1989**, *22*, 853.
- Alexander, S. *J. Phys. (Paris)* **1977**, *38*, 983.
- (a) Kent, M. S.; Lee, L. T.; Farnoux, B.; Rondelez, F. *Macromolecules* **1992**, *25*, 6240. (b) Factor, B. J.; Lee, L. T.; Kent, M. S.; Rondelez, F. *Phys. Rev. E* **1993**, *48*, 2354. (c) Kent, M. S.; Lee, L. T.; Factor, B. J.; Rondelez, F.; Smith, G. H. *J. Chem. Phys.* **1995**, *103*, 2320.
- (a) Bijsterbosch, H. D.; de Haan, V. O.; de Graaf, W.; Mellema, M.; Leermakers, F. A. M.; Cohen Stuart, M. A.; van Well, A. A. *Langmuir* **1995**, *11*, 4467. (b) Currie, E. P. K.; Leermakers, F. A. M.; Cohen Stuart, M. A.; Fleer, G. J. *Macromolecules* **1999**, *32*, 487.
- (a) Lai, P.-Y.; Halperin, A. *Macromolecules* **1991**, *24*, 4981. (b) Shim, D. F. K.; Cates, M. E. *J. Phys. (Paris)* **1989**, *50*, 3535.
- Flory, P. J. *Statistical Mechanics of Chain Molecules*; John Wiley & Sons: New York, 1969.
- de Gennes, P. G. *Adv. Colloid Interface Sci.* **1987**, *27*, 189.

MA991988O